

The universal template is a subtemplate of the double-scroll template

This article has been downloaded from IOPscience. Please scroll down to see the full text article.

2013 J. Phys. A: Math. Theor. 46 065102

(<http://iopscience.iop.org/1751-8121/46/6/065102>)

View [the table of contents for this issue](#), or go to the [journal homepage](#) for more

Download details:

IP Address: 129.25.7.39

The article was downloaded on 30/01/2013 at 14:25

Please note that [terms and conditions apply](#).

The universal template is a subtemplate of the double-scroll template

Christophe Letellier¹ and Robert Gilmore²

¹ CORIA UMR 6614, Université de Rouen, Av de l'Université, BP 12, F-76801 Saint-Etienne du Rouvray Cedex, France

² Physics Department, Drexel University, Philadelphia, PA 19104, USA

E-mail: Christophe.Letellier@coria.fr

Received 16 July 2012, in final form 12 December 2012

Published 29 January 2013

Online at stacks.iop.org/JPhysA/46/065102

Abstract

The double-scroll attractor that can be produced by a wide class of nonlinear electronic circuits is known to contain periodic orbits of all types under certain operating conditions. We identify the branched manifold that describes the double-scroll attractor under these operating conditions. We then show that Ghrist's universal template is embedded as a subtemplate in the double-scroll template.

PACS number: 05.45.—

(Some figures may appear in colour only in the online journal)

1. Introduction

In 1983 Birman and Williams proved a theorem [1] that provides a strong connection between an important class of chaotic dynamical systems $\dot{\mathbf{x}} = \mathbf{f}(\mathbf{x}; \mathbf{c})$, (where $\mathbf{x} \in \mathbb{R}^3$ is the state vector and \mathbf{c} the set of parameter values) and some relatively simple topological structures called branched manifolds (also known as knot-holders or templates). Using this theorem they were able to classify all the knots that appear in the geometric Lorenz attractor [2], and which exist as periodic orbits satisfying the Lorenz equations [3] for certain parameter values [4]. Birman and Williams observed [2] that only a restricted class of knots are supported in the branched manifold that described the Lorenz attractor. They conjectured that no flow $f(x; c)$ could be found that supported every knot type [1].

In 1997, Ghrist [5] identified a relatively simple branched manifold with inversion symmetry that supported all knot and link types. Ghrist and Holmes [5, 6] also identified a flow that supported all knot and link types. This flow had been known for many years: it had been introduced by Chua *et al* [7] to describe an electronic circuit. This is one of a class of double-scroll attractors proposed earlier by Rössler [8] and found in various circuits [9–11] (see [12] for a review). The proof that the Chua equations support all knot and link types

for certain control parameter values was not directly related to Ghrist’s universal template. Rather, it depended on the properties of flows in the neighborhood of a Shil’nikov connection [13, 14]. As a consequence, no direct relation was proposed between a template describing the topology of the double-scroll attractor and the universal template proposed by Ghrist and Holmes. Our objective is therefore to propose a template for the double-scroll attractor and then to establish how the universal template is related to that template. The subsequent part of this paper is organized as follows. Section 2 is devoted to the extraction of a template for the double-scroll attractor discussed by Ghrist and Holmes. How Ghrist’s universal template is related to the template of the double-scroll attractor is explained in section 3. Section 4 provides a discussion and some conclusions.

2. The double-scroll attractor and its template

The Chua circuit is described by the flow [7]

$$\begin{cases} \dot{x} = \alpha (y - \phi(x)) \\ \dot{y} = x - y + z \\ \dot{z} = -\beta y, \end{cases} \quad (1)$$

where

$$\phi(x) = m_1 x - \frac{1}{2}(m_0 - m_1) (|x + 1| - |x - 1|) = -\phi(-x) \quad (2)$$

and $m_0 = \frac{5}{7}$ and $m_1 = \frac{2}{7}$. These equations have a fixed point at the origin and a symmetric pair of fixed points at $\pm(x_0, 0, -x_0)$, where $x_0 = (m_0/m_1) - 1$ when $m_0 > 2m_1 > 0$.

Ghrist and Holmes have shown that when $\alpha = 7$ these equations have solutions supporting every knot and link type for $6.5 \leq \beta \leq 10.5$. Their proof depends on four properties that are satisfied by these equations for the parameter range given.

- (1) The equations are equivariant under inversion symmetry.
- (2) The fixed point at the origin is a focus with eigenvalues $\{\lambda_s \pm i\omega, \lambda_u\}$, with

$$\lambda_u > -\lambda_s > 0. \quad (3)$$

- (3) There is a homoclinic connection at the origin.
- (4) The homoclinic cycle is unknotted.

A template was proposed for a double-scroll attractor solution to the Chua circuit (1), but for different parameter values ($m_0 = -\frac{8}{7}, m_1 = -\frac{7}{9}, \alpha = 9$ and $\beta = \frac{100}{7}$) [15]. The template of another double-scroll attractor produced by an electronic circuit rather similar to the Chua circuit was proposed in [16]. These parameter values do not correspond to the values for which the four previous conditions were proved. We therefore constructed the branched manifold that describes the double-scroll attractor obtained with the parameter values used by Ghrist and Holmes [6], that is, by those used by Chua *et al* [7] by integrating equations (1). The chaotic solution to these equations for $\alpha = 7, \beta = 9$ is shown in figure 1.

For convenience the attractor is shown in the (z, \dot{z}) projection of a differential coordinate system (z, \dot{z}, \ddot{z}) related to the original coordinate system (x, y, z) by a constant nonsingular transformation with determinant $-\beta^2$. It is convenient to choose as a Poincaré section the union of two disks. These are shown as dark lines extending outward from the unstable foci at $(\pm\frac{3}{2}, 0, 0)$ (figure 1). These two disks are defined according to

$$P \equiv \{(z_n, \dot{z}_n) \in \mathbb{R}^3 | \dot{z}_n = 0, \ddot{z}_n > 0, z_n < -\frac{3}{2}\} \cup \{(z_n, \dot{z}_n) \in \mathbb{R}^3 | \dot{z}_n = 0, \ddot{z}_n < 0, z_n > +\frac{3}{2}\}. \quad (4)$$

In order to compute an adequate first-return map, distances along the branch line in each component have to be measured from inside to outside [17]. Then, distances are normalized to

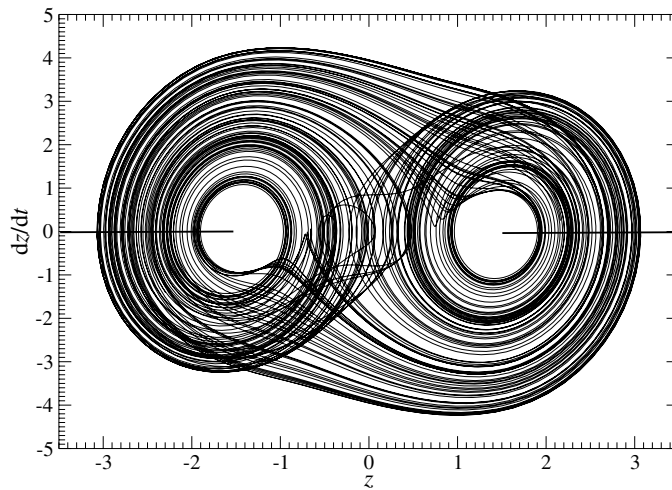


Figure 1. Chaotic attractor solution to the Chua equations (1). Parameter values: $\alpha = 7$, $\beta = 9$.

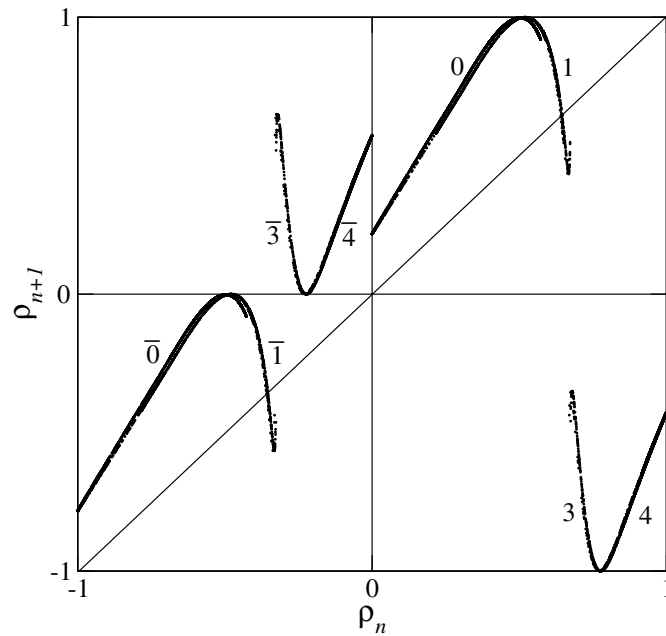


Figure 2. First-return map to a two-component Poincaré section of the chaotic attractor solution to the Chua equations (1). Parameter values: $\alpha = 7$ and $\beta = 9$.

the unit interval to optimize the picture. The left component is shifted by -1 to distinguish it from the right component. The first-return map thus obtained is shown in figure 2. Increasing (decreasing) branches are associated with order preserving (reversing) branches, that is, with an even (odd) number of π -twists. Four branches are obtained in each component. There are some branches which are not very often visited between branch $\bar{1}$ (1) and branch $\bar{3}$ (3): they will be neglected in this study.

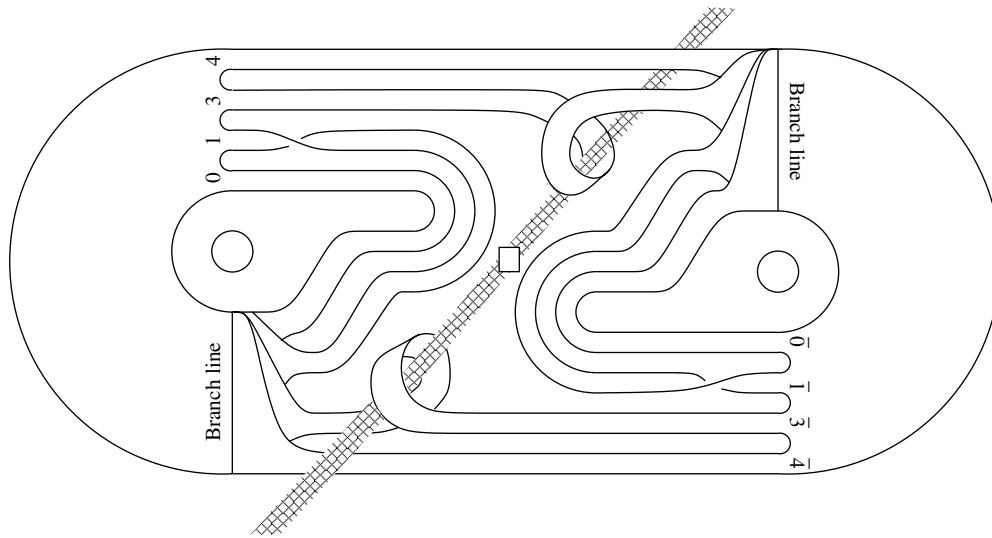


Figure 3. Branched manifold that describes the double-scroll attractor shown in figure 1.

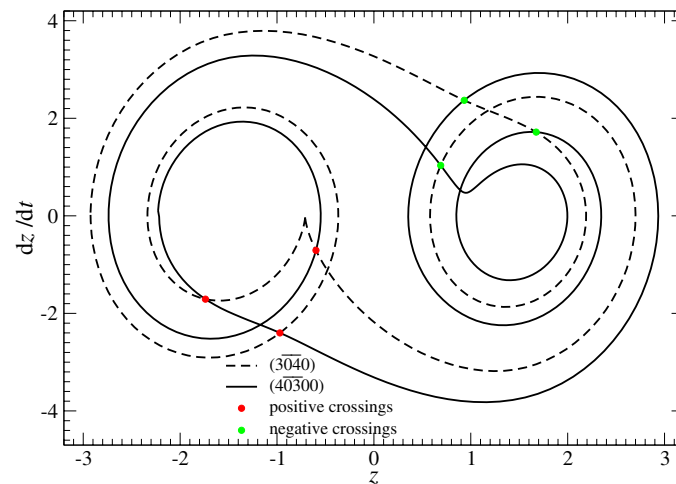


Figure 4. Two unstable periodic orbits extracted from the chaotic attractor solution to the Chua equations (1). Their orbital sequences are (3040) and (40300). The linking number between these two periodic orbits is null. Parameter values: $\alpha = 7$ and $\beta = 9$.

After many visual inspections in a three-dimensional representation of the attractor, we found that this chaotic attractor can be described by the branched manifold shown in figure 3. This branched manifold has two branch lines. The number of π -twists is null for branches $\bar{0}$, $\bar{4}$, $\bar{0}$ and $\bar{4}$, and odd for branches $\bar{1}$, $\bar{3}$, $\bar{1}$ and $\bar{3}$. Branches $\bar{1}$ and $\bar{3}$ carry negative twist (using the right hand convention) and branches $\bar{1}$ and $\bar{3}$ carry positive twist.

We checked that the linking numbers predicted by this template are in agreement with those computed from the unstable periodic orbits extracted from the chaotic attractors using a close return method. An example is shown in figure 4 with the knot made of the period-4 orbit ($\bar{3040}$) and of the period-5 orbit ($\bar{40300}$). The corresponding linking number

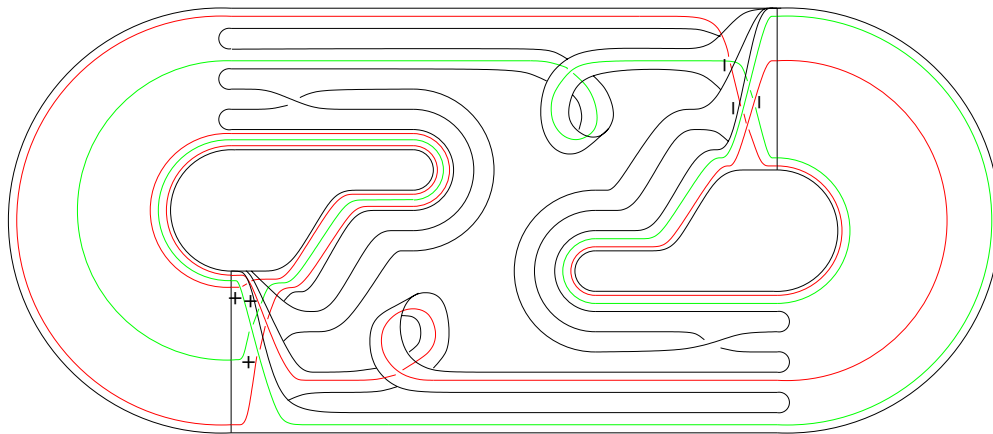


Figure 5. Branched manifold that describes the double-scroll attractor shown in figure 1.

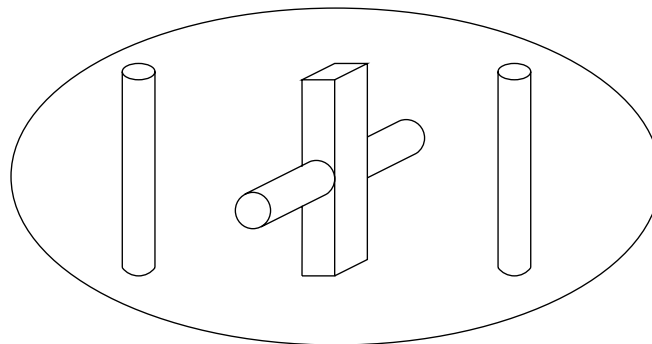


Figure 6. Sketch of the holes associated with the bounding torus of the double-scroll attractor.

$lk(\overline{3040}, \overline{40300}) = \frac{1}{2}(+3 - 3) = 0$ as obtained in a template construction (figure 5). Our template thus describes the relative organization of most of the periodic orbits embedded within the attractor for $\alpha = 7$ and $\beta = 9$ (we did not consider orbits having periodic points in the branches between branch $\bar{1}$ (1) and branch $\bar{3}$ (3)).

It is possible to determine the genus of the torus bounding the attractor as follows. A bounding torus is a semi-permeable closed surface surrounding the attractor. This surface has some holes whose number defines the genus [18]. In the present case, there are three fixed points, one saddle point located at the origin of the phase space and two symmetry-related foci; they are represented in figure 3 by a square and two small circles, respectively. In the case of the double-scroll, there is one additional hole which is defined by the axis around which the trajectory spirals in the middle of the attractor and which is sketched as the gray band in figure 3. From the bounding torus point of view, this hole crosses the hole associated with the saddle point, leading to the bounding torus sketched in figure 6.

Using a decomposition of the bounding torus in plaquets as performed in [19] (see appendix therein) and using the Euler–Poincaré index

$$V - E + F = 2 - 2g, \tag{5}$$

where (E, V, F) are the numbers of vertices, edges and faces, it was found that the genus of the bounding torus is equal to five. An alternative way of seeing this was presented in [19].

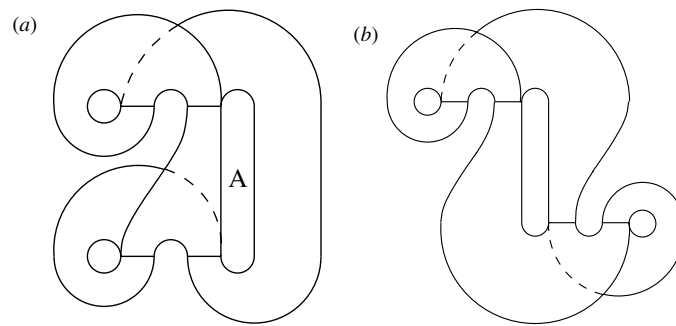


Figure 7. (a) Universal template as drawn by Ghrist [5, 6]. If the lower branch line is moved around from the 7 o'clock position to the 5 o'clock position the inversion symmetry of this template becomes apparent (b).

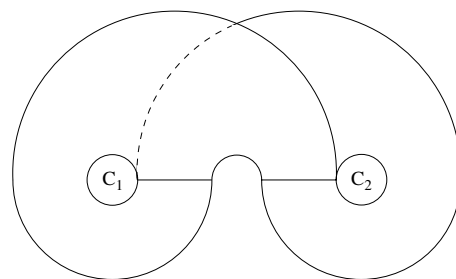


Figure 8. This $2 \downarrow 1$ image of the universal template is obtained by modding out [17] the inversion symmetry. The Lorenz template is itself invariant under rotations about the vertical axis.

Briefly, enlarge the hole at the intersection of the cylindrical and square cylinders, place your thumbs in one of the round holes in the surface, and turn the structure inside out, and project onto a plane. The hole with the thumbs in it will turn into a projection of the outer boundary of a torus pierced by five holes, three round holes separated by two square holes (cf figure 11 below).

3. Ghrist's universal template

A simple universal template as drawn by Ghrist has the form shown in figure 7. Crossings in the two 'ears' have opposite signs. Interchanging the two ears is equivalent to a π phase shift around the interior region labeled A. As shown in figure 8, the $2 \downarrow 1$ image of the universal template obtained by modding out [17] the inversion symmetry is the Lorenz template.

We now show that the Ghrist universal template shown in figure 7 occurs as a subtemplate of the double-scroll template shown in figure 3. The steps are shown in figure 9. First we construct a subtemplate by removing the four twisted branches and retaining only the four untwisted branches. Then we rotate the upper branch line from the 11 o'clock position to the 1 o'clock position. The result is shown in figure 9(a). Next we move the return flow AB from the left to the right. The resulting subtemplate, shown in figure 9(b), is the universal template, shown in figure 7.

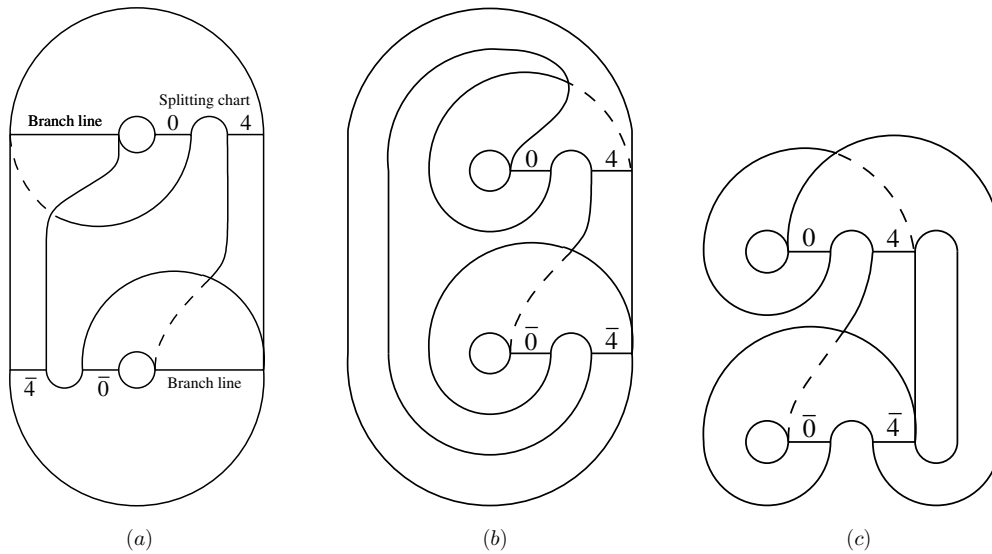


Figure 9. A subtemplate is constructed from the double-scroll template by removing the four branches with a twist (a). The upper branch line is identified with the upper splitting chart and the bottom splitting chart is identified with the bottom branch line (b). Branch 4 is moved from the left to the right (c), yielding a subtemplate equivalent to the universal template shown in figure 7.

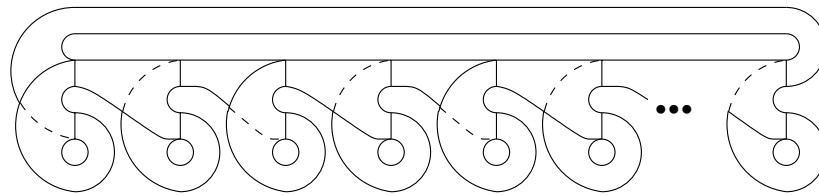


Figure 10. Class of templates obtained by renormalization of the Ghrst universal template.

The class of templates introduced in [5, 6] and shown in figure 10 (called \mathcal{W}_q in [5, 6]) can be obtained in a similar way. If the template is modified to a circular form and the $2q$ ‘ears’ are equally spaced around the circle, it is clear that \mathcal{W}_q is a q -fold cover of the universal template with C_q symmetry. Equivalently, it is a $2q$ -fold cover with S_{2q} symmetry [17] of a Lorenz template. The image Lorenz template has rotation symmetry and the axis around which the cover is constructed passes through either of the foci of the Lorenz template.

4. Discussion

We have constructed a branched manifold that describes the double-scroll attractor obtained for parameter values for which the Ghrst and Holmes theorem was proved. We then showed that the universal template of Ghrst is a subtemplate of the double-scroll template obtained by retaining only the untwisted branches in figure 3. This construction provides an alternative way of seeing that the double-scroll attractor contains knots and links of all types. Ghrst’s universal template thus describes the relative organization of a subset of the unstable periodic orbits embedded within the double-scroll attractor.

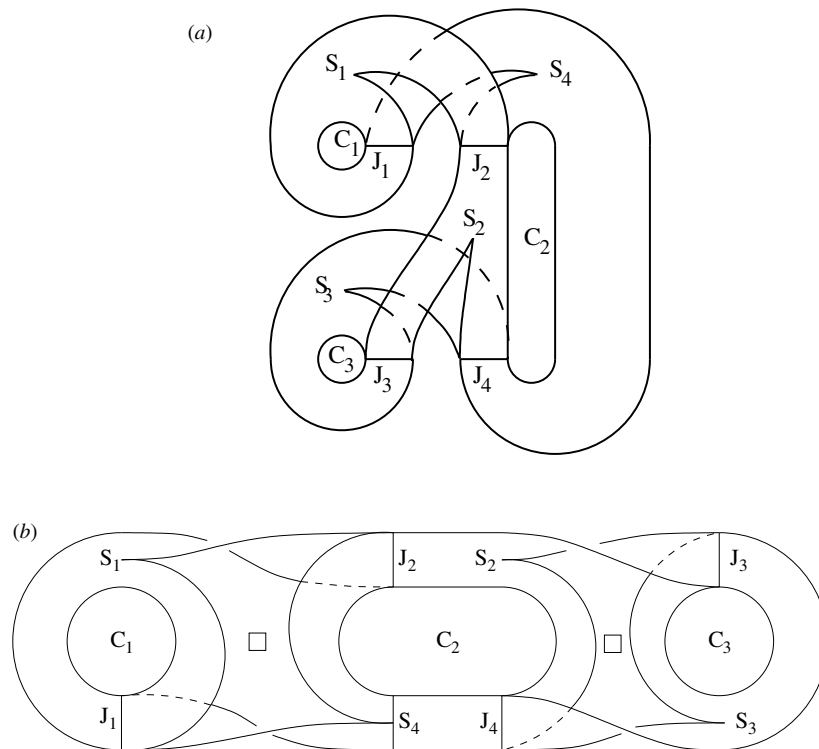


Figure 11. Representation of the universal template as embedded in a bounding torus of genus five. The two holes surrounding the saddle points are represented by two squares. The three other holes surround the foci C_i ($i = 1, 2, 3$).

Ghrist’s universal template possesses an inversion symmetry and an order-2 rotation symmetry, as do the double-scroll equations (1). Modding out the inversion symmetry leads to a Lorenz branched manifold. This branched manifold has rotation symmetry. Modding out this symmetry leads to a branched manifold [20] of the type that supports the flow on the well-known Rössler attractor [21]. Working backward, we can construct the universal template in two steps from well-known templates. First, lift the Rössler template to a two-fold cover with rotation symmetry around an axis between the two branches of the template. See figure 5 b in [22]. Second, lift the resulting Lorenz attractor to a two-fold cover with inversion symmetry through either of the two foci. See figure 6.35c in [17]. An alternative representation of the universal template is provided in figure 11. In this standard representation it is clear that the universal template is of genus-five type [18], three holes surrounding foci and two holes surrounding saddle points.

Acknowledgments

One of the authors (RG) thanks the US National Science Foundation for support under grant NSF PHY-0754081.

References

- [1] Birman J and Williams R F 1983 Knotted periodic orbits in dynamical systems-II: knot holders for fibred knots *Contemp. Math.* **20** 1–60

- [2] Birman J and Williams R F 1983 Knotted periodic orbits in dynamical systems-I: Lorenz's equations *Topology* **22** 47–82
- [3] Lorenz E N 1963 Deterministic nonperiodic flow *J. Atmos. Sci.* **20** 130–41
- [4] Sparrow C 1982 *The Lorenz Equations: Bifurcations, Chaos and Strange Attractors (Applied Mathematical Sciences vol 41)* (Berlin: Springer)
- [5] Ghrist R W 1997 Branched two manifolds supporting all links *Topology* **36** 423–48
- [6] Ghrist R W and Holmes P J 1996 An ODE whose solutions contain all knots and links *Int. J. Bifurcation Chaos* **6** 779–800
- [7] Chua L, Komuro M and Matsumoto T 1986 The double-scroll family *IEEE Trans. Circuits Syst.* **33** 1072–118
- [8] Rössler O E 1977 Chemical turbulence: a synopsis *Synergetics: Proceedings of the International Workshop on Synergetics at Schloss Elmau (Bavaria, 2–7 May, 1977)* ed H Haken (New York: Springer) pp 174–83
- [9] Pikovskii A S and Rabinovich M I 1978 A simple autogenerator with stochastic behavior *Sov. Phys.—Dokl.* **23** 183–5
- [10] Arnéodo A, Coulet P and Tresser C 1981 Possible new strange attractors with spiral structure *Commun. Math. Phys.* **79** 573–9
- [11] Brockett R F 1982 On conditions leading to chaos in feedback systems *Proc. 21st IEEE Conf. on Decision and Control* **vol 2** pp 932–6
- [12] Letellier C and Ginoux J-M 2009 Development of the nonlinear dynamical systems theory from radio engineering to electronics *Int. J. Bifurcation Chaos* **19** 2131–63
- [13] Shil'nikov L P 1965 A case of existence of a countable number of periodic motions *Sov. Math.—Dokl.* **6** 163–6
- [14] Shil'nikov L P 1970 A contribution to the problem of the structure of an extended neighborhood of a rough equilibrium state of saddle-focus type *Math. USSR Sb.* **10** 91–102
- [15] Kocarev L, Tasev Z and Dimovski D 1994 Topological description of a chaotic attractor with spiral structure *Phys. Lett. A* **190** 399–402
- [16] Letellier C, Gouesbet G and Rulkov N 1996 Topological analysis of chaos in equivariant electronic circuits *Int. J. Bifurcation Chaos* **6** 2531–55
- [17] Gilmore R and Letellier C 2008 *The Symmetry of Chaos* (Oxford: Oxford University Press)
- [18] Tsankov T D and Gilmore R 2003 Strange attractors are classified by bounding tori *Phys. Rev. Lett.* **91** 134104
- [19] Letellier C and Gilmore R 2009 Poincaré sections for a new three-dimensional toroidal attractor *J. Phys. A: Math. Theor.* **42** 015101
- [20] Letellier C, Dutertre P and Maheu B 1995 Unstable periodic orbits and templates of the Rössler system: toward a systematic topological characterization *Chaos* **5** 271–82
- [21] Rossler O E 1976 An equation for continuous chaos *Phys. Lett. A* **57** 397–8
- [22] Letellier C and Gilmore R 2001 Covering dynamical systems: two-fold covers *Phys. Rev. E* **63** 16206